



Contents lists available at ScienceDirect

# Process Safety and Environmental Protection

journal homepage: [www.journals.elsevier.com/process-safety-and-environmental-protection](http://www.journals.elsevier.com/process-safety-and-environmental-protection)

## Brewery spent grain valorization through fermentation: Targeting biohydrogen, carboxylic acids and methane production

Jacobo Pérez-Barragán<sup>a,b</sup>, Cristina Martínez-Fraile<sup>b,c</sup>, Raúl Muñoz<sup>b,c</sup>, Guillermo Quijano<sup>d</sup>, Rafael Maya-Yescas<sup>e</sup>, Elizabeth León-Becerril<sup>a</sup>, Roberto Castro-Muñoz<sup>f</sup>, Octavio García-Depraect<sup>b,c,\*</sup>

<sup>a</sup> Department of Environmental Technology, Centro de Investigación y Asistencia en Tecnología y Diseño del Estado de Jalisco, A. C. Av. Normalistas 800, Colinas de la Normal, Guadalajara, Jalisco 44270, Mexico

<sup>b</sup> Institute of Sustainable Processes, University of Valladolid, Dr. Mergelina s/n., Valladolid 47011, Spain

<sup>c</sup> Department of Chemical Engineering and Environmental Technology, University of Valladolid, Dr. Mergelina s/n., Valladolid 47011, Spain

<sup>d</sup> Laboratory for Research on Advanced Processes of Water Treatment, Instituto de Ingeniería, Unidad Académica Juriquilla, Universidad Nacional Autónoma de México, Blvd. Juriquilla 3001, Querétaro 76230, Mexico

<sup>e</sup> Faculty of Chemical Engineering, Universidad Michoacana de San Nicolás de Hidalgo, Ciudad Universitaria, Morelia, Michoacán de Ocampo 58030, Mexico

<sup>f</sup> Department of Sanitary Engineering, Faculty of Civil and Environmental Engineering, Gdansk University of Technology, G. Narutowicza St. 11/12, Gdansk 80-233, Poland

### ARTICLE INFO

#### Keywords:

Acidogenic fermentation  
Biogas  
Dark fermentation  
Organic acids  
Lignocellulosic waste

### ABSTRACT

This study investigated three different fermentation approaches to explore the potential for producing biohydrogen, carboxylic acids, and methane from hydrolysates of thermally dilute acid pretreated brewer's spent grains (BSG). Initially, the research focused on maximizing the volumetric hydrogen production rate (HPR) in the continuous dark fermentation (DF) of BSG hydrolysates by varying the hydraulic retention time (HRT). The highest HPR reported to date of 5.9 NL/L-d was achieved at 6 h HRT, with a *Clostridium*-dominated microbial community. The effect of the operational pH (4, 5, 6, and 7) on the continuous acidogenic fermentation was then investigated. A peak carboxylic acid concentration of 17.3 g CODEquiv./L was recorded at pH 6, with an associated volumetric productivity of 900.5 ± 13.1 mg CODEquiv./L-h and a degree of acidification of 68.3 %. Lactic acid bacteria such as *Limosilactobacillus* and *Lactobacillus* were dominant at pH 4–5, while *Weissella*, *Enterococcus*, and *Lachnoclostridium* appeared at pH 6 and 7. Finally, this study evaluated the biochemical methane potential of the DF broth and the unfermented hydrolysates and found high methane yields of 659 and 517 NmL CH<sub>4</sub>/g-VS<sub>added</sub>, respectively, both within one week. Overall, the results showed that pretreated BSG can be a low-cost feedstock for the production of bioenergy and valuable bio-based chemicals in a circular economy.

### 1. Introduction

Brewing is one of the largest sectors of the global beverage industry. In 2021, global beer consumption reached approximately 185.6 million kiloliters, with a projected annual growth rate of 4.0 % (Holdings, 2021). Throughout the beer production process, various by-products are generated, including hot trub, brewer's yeast, and brewer's spent grains (BSG) (Rachwał et al., 2020). BSG, the most abundant solid waste produced during the mashing stage, accounts for up to 85 % of total brewery by-products (Hejna et al., 2021; Rachwał et al., 2020). On average, about 27 kg of BSG are generated per hectoliter of beer produced

(Wagner et al., 2022). In 2022, China, the world's leading beer producer, generated more than 2.3 million tons of BSG, while European countries together produced about 2.6 million tons of this waste (Statista Search Department, 2022). Given its composition (protein 20–24 %, cellulose 26–60 %, hemicellulose 19–60 %, lignin 13–56 %), the predominant current use for most BSG is as animal feed. However, this scenario provides an opportunity to explore new alternative valorization approaches with improved profitability (Pabbathi et al., 2022). Therefore, a higher economic value could be achieved by establishing a circular green process for BSG management through biotechnological processes.

Due to its abundant availability and favorable physicochemical

\* Corresponding author at: Department of Chemical Engineering and Environmental Technology, University of Valladolid, Dr. Mergelina s/n., Valladolid 47011, Spain

E-mail address: [octavio.garcia@uva.es](mailto:octavio.garcia@uva.es) (O. García-Depraect).

<https://doi.org/10.1016/j.psep.2024.08.071>

Received 19 May 2024; Received in revised form 12 August 2024; Accepted 19 August 2024

Available online 30 August 2024

0957-5820/© 2024 The Author(s). Published by Elsevier Ltd on behalf of Institution of Chemical Engineers. This is an open access article under the CC BY-NC-ND license (<http://creativecommons.org/licenses/by-nc-nd/4.0/>).

### Nomenclature

<b>BMP</b>	Biochemical methane potential
<b>BSG</b>	Brewer's spent grain
<b>COD</b>	Chemical oxygen demand
<b>CODequiv</b>	Chemical oxygen demand equivalents
<b>DF</b>	Dark fermentation
<b>HMF</b>	5-hydroxymethylfurfural
<b>HPR</b>	Hydrogen production rate
<b>HPSI</b>	Hydrogen production stability index
<b>HRT</b>	Hydraulic retention time
<b>YH<sub>dry-BSG</sub></b>	Net hydrogen production per mass of dry BSG
<b>HY</b>	Hydrogen yield
<b>OLR</b>	Organic loading rate
<b>SCOD</b>	Soluble chemical oxygen demand
<b>TCOD</b>	Total chemical oxygen demand
<b>TN</b>	Total nitrogen;
<b>TOC</b>	Total organic carbon
<b>TS</b>	Total solids
<b>VFA</b>	Volatile fatty acids
<b>VS</b>	Volatile solids
<b>VSS</b>	Volatile suspended solids

properties, BSG stands out as a promising lignocellulosic feedstock for the production of biofuels and marketable chemicals. Numerous studies have investigated the potential of BSG for the production of various biofuels, such as ethanol (Alonso-Riaño et al., 2022; Wagner et al., 2022), butanol (Fernández-Delgado et al., 2019; Giacobbe et al., 2019), methane (Buller et al., 2022; Lins et al., 2023), hydrogen (Sganzerla et al., 2023; Sarkar et al., 2022), and other value-added compounds such as volatile fatty acids (VFAs) (Liu et al., 2023). Hydrogen, recognized for its renewable and clean attributes with high energy content (142 kJ/g) and zero associated greenhouse gas emissions (García-Depraect et al., 2020; Sahrin et al., 2022), has been a focal point in BSG-based biofuel studies. A variety of microorganisms with different physiological and metabolic characteristics are involved in different biological methods for hydrogen production, including green algae, cyanobacteria, photosynthetic bacteria, and dark fermentative bacteria. These photosynthetic and non-photosynthetic microbes are capable of producing hydrogen gas through various metabolic pathways (Woon et al., 2023). Among the various biological processes for hydrogen production, dark fermentation (DF) is the most extensively studied due to its high production rates, compatibility with anaerobic digestion, and versatility in utilizing various organic wastes. As a result, numerous investigations have focused on the biogenic production of hydrogen from BSG (Li and Tao, 2016; Zhang and Zang, 2016; Soares et al., 2024). Despite significant scientific advances in the field, there are currently no continuous DF processes for BSG, highlighting the critical need for the design and evaluation of such systems.

In addition to its role in hydrogen production, acidogenic fermentation provides a pathway for the production of organic acids, including butyrate, acetate, propionate, and others. These short-chain carboxylic acids serve multiple purposes, including applications in wastewater treatment and as precursors for the synthesis of other valuable chemical compounds (Sarkar et al., 2021). The type and amount of organic acids produced are significantly influenced by various factors, with the operational pH standing out as one of the most critical process parameters (Liang and Wan, 2015). The optimal pH range for organic acid production is typically between 5 and 11, although the exact optimal pH is subject to variables such as the target product(s), the type of feedstock used, and the intricacies of the microbiological processes involved (Sarkar et al., 2021). Currently, there is limited research on the production of carboxylic acids from BSG (Teixeira et al., 2020; Guarda et al.,

2021; Liu et al., 2023). This knowledge gap is even more evident for continuous acidification studies. Furthermore, it is worth noting that understanding the microbiology of the acidogenic fermentation of BSG is crucial for optimizing the production of carboxylic acids. However, the microbiome involved in the continuous production of carboxylic acids from BSG is a research topic that has not been extensively studied.

Despite the numerous advantages of DF for hydrogen production, a notable limitation is the incomplete substrate utilization, with DF achieving a maximum theoretical hydrogen yield of 4 mol H<sub>2</sub>/mol hexose. This value represents only one-third of the energy content of hexose carbohydrates (Soares et al., 2024). An alternative strategy to improve the overall energy production yield is to utilize the DF effluent for additional biogas production through anaerobic digestion. For instance, Lins et al. (2023) reported the biochemical methane potential of BSG to be 580 NmL per gram of volatile solids (VS) added. However, to the best of the authors' knowledge, the fermentation broth derived from BSG DF has not been evaluated for biogas production. In line with advances in the lignocellulosic biorefinery industry, the present study aimed to evaluate three different biotechnological approaches to the valorization of the BSG resource. Specifically, the scientific objectives were i) to evaluate the effect of hydraulic residence time (HRT) on the continuous production of biohydrogen through the DF of BSG hydrolysates; ii) to evaluate the effect of pH on the continuous production of organic acids through the acidogenic fermentation of BSG hydrolysates; and iii) to evaluate the biochemical methane potential of fermented and raw BSG hydrolysates. In addition, the associated microbiology in the process of DF and acidogenic fermentation was also studied.

## 2. Materials and methods

### 2.1. Inocula

The two reactors dedicated to the production of hydrogen and carboxylic acids were inoculated with the same acidogenic inoculum (Regueira-Marcos et al., 2023). The primary source of this acidogenic inoculum was the digestate derived from a mesophilic pilot-scale anaerobic digester operating on food waste (Marín et al., 2022). In order to inhibit methanogenic communities, the digestate was subjected to a heat shock pretreatment (90 °C for 20 min). The resulting mixed culture was then enriched by successive subcultures utilizing lactose (10 g/L) as the sole carbon source. The composition of the growth medium was (in g/L) NH<sub>4</sub>Cl 2.4, K<sub>2</sub>HPO<sub>4</sub> 2.4, MgCl<sub>2</sub>·6 H<sub>2</sub>O 2.5, KH<sub>2</sub>PO<sub>4</sub> 0.6, CaCl<sub>2</sub>·2 H<sub>2</sub>O 0.15, and FeCl<sub>2</sub>·4 H<sub>2</sub>O 0.035 (García-Depraect et al., 2022). All reagents were of analytical grade. For the methane production potential tests, anaerobic sludge (19.6 g total solids (TS)/L, 11.4 g VS/L, pH 7.6) from a mesophilic digester used for municipal wastewater treatment in Valladolid, Spain, was used.

### 2.2. Preparation, characterization, and hydrolysis of BSG

BSG obtained from a local brewery was used without any preparatory steps, in order to evaluate the material under conditions that closely resemble its state immediately after the beer production process. For its preservation, BSG was packed in bags of about 2 kg and stored at –20 °C until its use. The physicochemical characterization of BSG, performed according to the National Renewable Energy Laboratory (NREL) procedures (Sluiter et al., 2008), is presented and discussed in Section 3.1.

The thawed BSG was subjected to acid-assisted thermal pretreatment according to the procedure described by Castilla-Archilla et al. (2021). A TS concentration of 7 % w/w of BSG was used for hydrolysis. Sulfuric acid with a purity of 96 % and a density of 1.84 g/mL, obtained from AppliChem (Germany), was used at a concentration of 1.5 % v/v to perform the acid hydrolysis. The hydrolysis process was performed in a 10 L borosilicate bottle, with a working volume of 5 L. The homogenized mixture was autoclaved (Raypa, Spain) at 121 °C for 20 min. At the end of the hydrolysis, the borosilicate bottle was cooled and then the

hydrolysate was filtered through a #20 sieve (850  $\mu\text{m}$ ) to separate the liquid fraction. The hydrolysate was then subjected to physicochemical characterization (see Section 3.1) and stored in a sterile glass bottle at 4  $^{\circ}\text{C}$  until further use.

### 2.3. Experimental setup and operating conditions for hydrogen production

The continuous hydrogen production reactor consisted of a polyvinyl chloride fermenter with a total volume of 1.2 L (0.4 L headspace). As shown in Fig. 1, the setup included a pH controller (BSV Electronic SL, Spain) along with a pH probe (HO35-BSV01, Spain) and included sampling ports for both gas and liquid phases. A continuous gas flow meter was also incorporated into the system. Prior to inoculation of the reactor, 0.1 L of the acidogenic inoculum was activated in a 2.1 L gas-tight fermenter for 24 h at  $37 \pm 1^{\circ}\text{C}$  and approximately 150 rpm, without pH control (initial pH 6.4). This activation was performed using 0.9 L of a mineral growth medium supplemented with 10 g/L lactose, as described in Section 2.1. Initially, the reactor was inoculated with 10 % v/v of the fresh and active inoculum at a volatile suspended solids (VSS) concentration of 0.46 g/L and operated in batch mode for 8 h before transitioning to continuous operation. The continuous operation lasted for 12.5 days and was divided into three operation stages (I–III). These stages had decreasing HRTs of 12, 9, and 6 h, respectively, resulting in organic loading rate (OLR) values of 44.2, 59.0, and 88.5 g chemical oxygen demand (COD)/L-d, respectively (Table 1). Throughout the operation, the reactor was maintained at  $37 \pm 1^{\circ}\text{C}$  in a temperature-controlled chamber. The system was magnetically agitated at approximately 300 rpm and the pH was maintained at  $6.0 \pm 0.1$  using 6 M NaOH. Samples were taken periodically from both the influent and effluent to assess the organic acid profile and the efficiency of total carbohydrate and COD removal. In addition, the volumetric flow rate and composition of the off-gas produced during DF were measured. The volume of hydrogen was normalized to standard volume units (NmL or NL) under standard pressure and temperature conditions (0  $^{\circ}\text{C}$  and 1 atm). The evaluation of the DF process included parameters such as volumetric hydrogen production rate (HPR), hydrogen yield (HY), hydrogen purity, organic acid profiles, and microbial community composition. To distinguish between stable and unstable operation, a

**Table 1**

Duration and conditions of operation of the reactor for the continuous production of hydrogen.

Parameter	Process stage		
	I	II	III
HRT (h)	12	9	6
OLR (g COD/L-d)	44.2	59.0	88.5
Time (days)	0–4.5	4.5–9	9–12.5
HRT cycles	9	12	14

OLR: organic loading rate.

HRT: hydraulic retention time.

COD: chemical oxygen demand.

dynamic stability index was also introduced (Eq. 1) (García-Depraect et al., 2020). Process stability was defined as achieving a HPSI consistently equal to or greater than 0.8 for at least three consecutive cycles.

$$HPSI = 1 - \frac{\text{standard deviation HPR}}{\text{average HPR}} \quad (\text{Eq. 1})$$

The effluent collected at a HRT of 6 h (which was determined to be the optimal HRT for hydrogen production) was used for subsequent biogas evaluation in biochemical methane potential (BMP) tests.

### 2.4. Experimental design and operating parameters for carboxylic acids production

Continuous operation for the production of organic acids followed the same reactor setup procedure as previously described for hydrogen production. A Vernier sensor connected to a LabQuest Mini multi-channel data acquisition interface (Vernier Software & Technology, USA) was used for pH control. The start-up strategy consisted of inoculating the reactor in batch mode with an initial pH adjustment of  $\sim 7$  to allow the microbial communities to adapt to the substrate prior to the continuous strategy. In the continuous mode for organic acid production, a HRT of 24 h was used and the pH was gradually adjusted from 4 to 5, 6, and 7 using 6 M NaOH as the alkali agent (Fig. 1). The reactor was operated continuously for 50 days, divided into four operating stages (I–IV; see Table 2). Throughout the operation, influent and effluent samples were collected for subsequent analysis. Simultaneously,

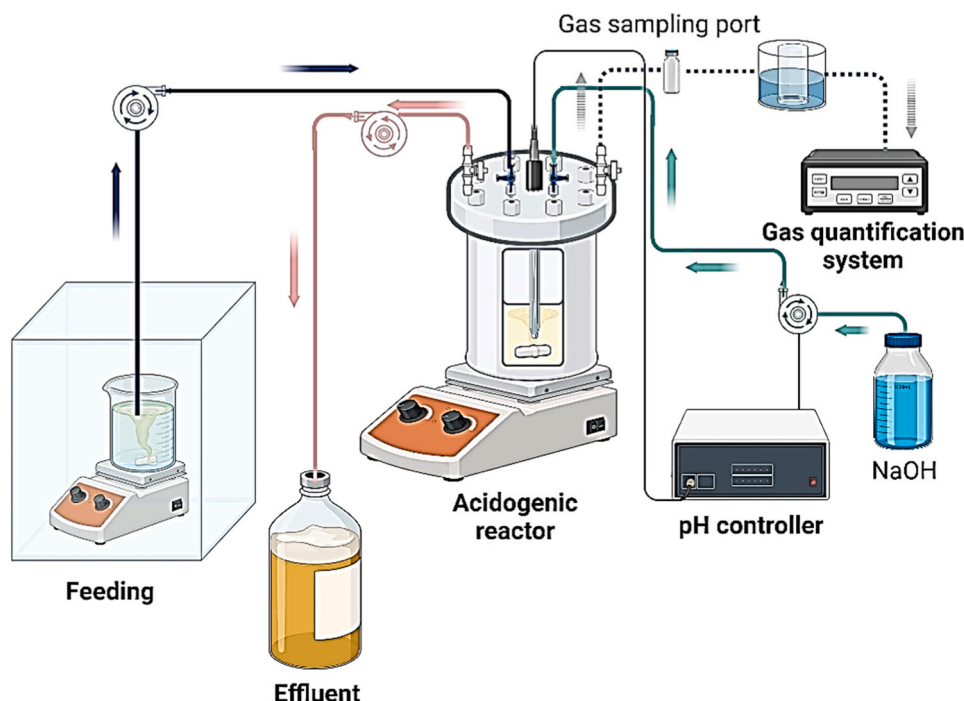


**Fig. 1.** Schematic diagram of the reactor setup used to produce hydrogen and carboxylic acids.

**Table 2**

Duration and conditions of operation of the reactor for the continuous production of carboxylic acids.

Parameter	Process stage			
	I	II	III	IV
pH	4	5	6	7
Time (days)	0–13	13–26	26–38	38–50
HRT (h)	24	24	24	24
OLR (g COD/L-d)	31.6	31.6	31.6	31.6

OLR: organic loading rate.

HRT: hydraulic retention time.

COD: chemical oxygen demand

the flow rate and composition of the gas stream were monitored.

The degree of acidification (in %) was quantified using Eq. (2), where CODEquiv. is the cumulative sum of COD equivalents (in g/L) of all organic acids measured at pseudo-steady state over different pH conditions, and COD<sub>initial</sub> stands for the initial total COD concentration (in g/L) of the feedstock.

$$\text{Acidification degree}(\%) = \frac{\text{CODEquiv. effluent}}{\text{COD}_{\text{initial}}} * 100 \quad (2)$$

### 2.5. Biochemical methane production tests

The effluent collected from the hydrogen production reactor (operating at a HRT of 6 h) was used to conduct BMP tests. Raw BSG acid hydrolysate was also tested for comparison. These tests were performed in triplicate using anaerobic sludge alone as a blank to correct for endogenous methane production. Gas-tight reactors with a total volume of 2.1 L and a working volume of 500 mL were used for the BMP assays. A food to microorganism (F/M) ratio of 0.5 (based on VS) was maintained. All assays were performed under uniform conditions, maintaining a temperature of 37 °C with continuous agitation at 4 rpm using a roller bottle incubator (Scientific Products, USA). Prior to the start of the assays, the anaerobic sludge was preincubated at 37 °C for 7 days to minimize endogenous biogas production and then supplemented with sodium bicarbonate (5 g/L) as a buffering agent. To ensure anaerobic conditions, the sealed reactors were purged with pure helium gas for 1 min prior to the start of the assays. The assays were run for 12 days until biogas production ceased, as indicated by stabilization of the cumulative methane production curves. Daily measurements of biogas production were recorded using the standard manometric method (García-Depraect et al., 2022). Methane yield was determined as the volume of methane per gram of VS added and the volume of methane per gram of dry BSG. The temporal pattern of methane yield was characterized using the modified Gompertz model described by Eq. (3) (Diaz-Cruces et al., 2020). In this equation,  $H(t)$  represents the total amount (in mL) of methane produced at culture time  $t$  (in days), while  $H_{\text{max}}$  represents the maximum cumulative amount (in mL) of methane produced.  $R_{\text{max}}$  is the maximum methane production rate (in mL/day), and  $\lambda$  is the lag time (in days). Finally, at the end of the experiment, samples of the digestate were collected for the analysis of pH and VFAs.

$$H(t) = H_{\text{max}} \cdot \exp \left\{ - \exp \left[ \frac{R_{\text{max}} \cdot 2.71828}{H_{\text{max}}} \cdot (\lambda - t) + 1 \right] \right\} \quad (3)$$

### 2.6. Analytical procedures

Sugars (i.e., glucose, xylose), inhibitors (i.e., furfural, 5-hydroxymethylfurfural), and organic acid concentrations were analyzed by high-performance liquid chromatography (HPLC) on a Shimadzu system (LC-2050 C, Japan) equipped with a refractive index detector (RID-20A, Japan) and with an ultraviolet detector (214 nm). For sugar analysis, a Rezex chromatographic column (RHM-Monosaccharide H+, Phenomenex, Germany) was used with the column temperature maintained at

60 °C and an eluent flow rate of 0.6 mL/min (5 mM H<sub>2</sub>SO<sub>4</sub>). Organic acids and inhibitors were analyzed using an Aminex HPX-87 H chromatographic column (Bio-Rad, USA) at a column temperature of 75 °C, with an eluent of 25 mM H<sub>2</sub>SO<sub>4</sub> at 0.7 mL/min flow rate. Gas composition was determined by gas chromatography using an Agilent GC system (8860-GC, USA) equipped with a thermal conductivity detector and a Varian CP-Molsieve 5 A Capillary Column (15 m, 0.53 mm, 15 μm) interconnected with a Varian CP-PoreBOND Q Capillary Column (25 m, 0.53 mm, 10 μm); ultra-high purity helium gas was used as the carrier gas at a flow rate of 13 mL/min (García-Depraect et al., 2022). Total organic carbon (TOC) and total nitrogen (TN) were quantified using a Shimadzu TOC analyzer (TOC-VCSH, Japan) according to the manufacturer's recommendations. Solids, total acidity, and COD were determined according to standard methods (APHA, 2005). Total and reducing sugars in the hydrolysate were measured by the phenol-sulfuric acid method and the dinitrosalicylic acid (DNS) method, respectively. The microbial community structure of the hydrogen and organic acid production reactors during their pseudo-steady states was analyzed. DNA extraction was performed using a FastDNA SPIN kit (MP Biomedicals, USA) according to the manufacturer's protocol. The extracted DNA was then subjected to 16S ribosomal RNA (rRNA) gene amplicon sequencing at Novogene company (Novogene, UK). Briefly, PCR amplification of the 16S V4-V5 rRNA region was performed using the primer pair 515 F/907 R. The PCR products of appropriate size were selected by agarose gel electrophoresis. Equal amounts of PCR products from each sample were pooled, end-repaired, A-tailed, and further ligated with Illumina adapters. The library was checked with Qubit and real-time PCR for quantification, while a bioanalyzer was used for size distribution detection. Quantified libraries were pooled and sequenced on an Illumina paired-end platform. Amplicon Sequence Variants (ASVs) were generated using the DADA2 method. The annotation database was Silva 138.1.

## 3. Results and discussion

### 3.1. Physicochemical properties of raw BSG and BSG acid hydrolysates

The weight percentages of total lignin, cellulose, and hemicellulose were determined to be  $22.4 \pm 0.1$ ,  $18.7 \pm 0.1$ , and  $6.8 \pm 0.1$ ,

**Table 3**

Physicochemical characterization of raw BSG and acid hydrolysates obtained from BSG.

Parameter (% w/w on a dry basis)	Raw BSG	Parameter	BSG acid hydrolysate
Moisture	2.7	TCOD (g/L)	$22.1 \pm 1.9$
Ash	3.7	SCOD (g/L)	$19.2 \pm 0.8$
Total solids	97.4	TOC (g/L)	$12.5 \pm 0.5$
Acid-insoluble lignin	$18.2 \pm 0.1$	TN (g/L)	$0.7 \pm 0.0$
Acid-soluble lignin	$4.2 \pm 0.1$	Total solids (g/L)	$42.9 \pm 4.4$
Total lignin	$22.4 \pm 0.1$	Volatile solids (g/L)	$41.3 \pm 4.4$
Cellulose	$18.7 \pm 0.1$	Reducing sugars (g/L)	$18.5 \pm 0.6$
Hemicellulose	$6.8 \pm 0.1$	*COD yield (%)	$31.6 \pm 1.0$
		Furfural (g/L)	BDL
		5-HMF (g/L)	$0.01 \pm 0.001$

TCOD: Total chemical oxygen demand

SCOD: Soluble chemical oxygen demand

TOC: Total organic carbon

TN: Total nitrogen

HMF: 5-hydroxymethylfurfural

BDL: Below analytical detection limit (< 0.01 g/L).

\*Ratio of the TCOD concentration in the hydrolysates to the initial total solids concentration.



respectively (Table 3). Although other content fractions were not explicitly quantified in this investigation, reported mean values from other studies include protein at  $20.9 \pm 2.4$  and lipids at  $8.5 \pm 2.2$  (Zeko-Pivač et al., 2022). The cellulose and lignin values reported in this study are consistent with previous studies and fall within the typical ranges of 15–25 % for cellulose and 12–28 % for lignin (Patel et al., 2018; Rojas-Chamorro et al., 2020; Zeko-Pivač et al., 2022). However, the hemicellulose value in this work differs from the literature values, which generally range from 15 % to 30 % (Patel et al., 2018; Rojas-Chamorro et al., 2020; Zeko-Pivač et al., 2022). This discrepancy may be due to a possible underestimation of the hemicellulose fraction, as it was determined based on xylose quantification only, omitting other major pentoses such as arabinose. In this context, arabinose could represent about  $6.0 \pm 1.6$  % of the total composition of BSG on a dry basis (Zeko-Pivač et al., 2022).

Table 3 shows the characterization of the acid hydrolysates, which showed an organic matter content, expressed as total and soluble COD (TCOD and SCOD, respectively), of  $22.1 \pm 1.9$  and  $19.2 \pm 0.8$ , respectively. The COD yield, calculated as the ratio of TCOD in the hydrolysates to the TS concentration used (7 % w/w), was 31.6 %, approximately 1.5 times lower than the value reported by Castilla-Archilla et al. (2021), which served as the basis for the conditions in this study. This discrepancy might be attributed to variations in reaction volumes and initial raw material moisture conditions, which affect homogenization and mass transfer phenomena and result in decreased hydrolysis performance. Nevertheless, a solids recovery of 61.3 % is consistent with the 57.1 % reported by Rojas-Chamorro et al. (2020) under similar pretreatment conditions (110 °C, 2 % H<sub>2</sub>SO<sub>4</sub>, 10 min). In addition, a favorable carbon to nitrogen ratio of 18 was achieved, which is close to the optimal range of 20–30 for anaerobic bacterial growth (Salangsang et al., 2022), suggesting that BSG can be directly used as the sole substrate in anaerobic fermentation.

### 3.2. Performance evaluation of the hydrogen production reactor

The continuous operation of hydrogen production involved the continuous feeding of BSG hydrolysates at three different HRTs of 12, 9, and 6 h.

Variations in HRT significantly affected the efficiency of hydrogen production, as shown in Fig. 2 and detailed in Table 4. After two days of continuous operation, the microorganisms adapted to the BSG hydrolysate, resulting in increased and stabilized hydrogen production (data not shown). Biogas production rates were  $8.8 \pm 0.6$ ,  $10.6 \pm 0.4$ , and  $11.2 \pm 0.4$  NL/L-d for HRTs of 12, 9, and 6 h, respectively, with an average hydrogen content of approximately 52.0 % v/v (Table 4).

A shorter HRT resulted in an increase in HPR. Under pseudo-steady states, the HPR values were  $4.5 \pm 0.3$ ,  $5.4 \pm 0.2$ , and  $5.9 \pm 0.1$  NL H<sub>2</sub>/L-d for HRTs of 12, 9, and 6 h, respectively, representing a 20 % increase between stage I and stage II, a 9 % increase between stage II and stage III, and a substantial 31 % increase between stage I and stage III. In contrast to the increased HPR, the HY in terms of COD added decreased with longer HRT. The maximum HY was  $103.7 \pm 7.1$  NL H<sub>2</sub>/g COD<sub>added</sub> at 12 h HRT but decreased to  $92.0 \pm 2.8$  NL H<sub>2</sub>/g COD<sub>added</sub> and  $66.0 \pm 1.8$  NL H<sub>2</sub>/g COD<sub>added</sub> for 9 and 6 h HRT, respectively. This decrease may be attributed to the influence of the OLR/HRT ratio. Research by Kumar et al. (2016) demonstrated that the peak HPR occurred at 3 h HRT with an OLR of 120 g galactose/L-d, whereas at 6 h HRT, the OLR

**Table 4**  
Summary of the process performance indicators collected during the continuous fermentative process for hydrogen production from BSG hydrolysate.

Parameter	Process Stage		
	I	II	III
HRT (h)	12	9	6
HPR (NL H <sub>2</sub> /L-d)	$4.5 \pm 0.3$	$5.4 \pm 0.2$	$5.9 \pm 0.1$
HY (NmL H <sub>2</sub> /g-COD <sub>added</sub> )	$103.7 \pm 7.0$	$92.0 \pm 2.8$	$66.0 \pm 1.8$
YH <sub>dry-BSG</sub> (NL H <sub>2</sub> /kg dry BSG)	$32.8 \pm 2.2$	$29.0 \pm 0.9$	$20.8 \pm 0.6$
H <sub>2</sub> content (% v/v)	$51.9 \pm 0.1$	$51.6 \pm 0.5$	$52.0 \pm 1.1$
HPSI	0.93	0.93	0.97

HRT: hydraulic retention time.

HPR: hydrogen production rate.

HY: hydrogen yield.

YH<sub>dry-BSG</sub>: net hydrogen production per mass of dry BSG.

HPSI: Hydrogen production stability index.

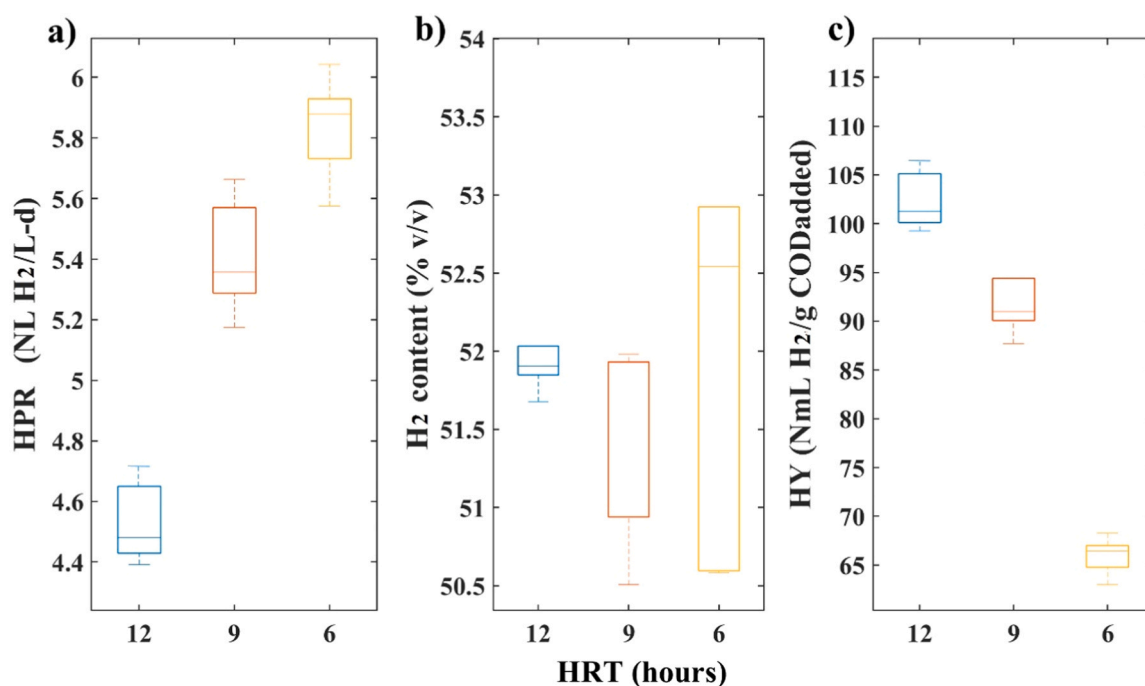


**Fig. 2.** Range of variation (quartiles and min-max range) for the volumetric hydrogen production rate (HPR) (a), hydrogen content (b), and hydrogen yield (HY) (c) during pseudo-stable conditions.

decreased to 60 g galactose/L-d, resulting in a maximum HY of 2.21 mol H<sub>2</sub>/mol galactose. Higher OLRs and lower HRTs favored certain hydrogen-producing bacteria such as *Clostridium* spp. while longer HRTs resulted in increased biomass retention and higher overall HY. While a comparative analysis with other studies is limited due to differences in operating modes and conditions, a comparison of the HPR in batch systems has been made. For example, Soares et al. (2024) worked with acid BSG hydrolysates with an initial pH of 7.5, 30 % inoculum, at 45 °C and showed a maximum HPR of 18.2 NL H<sub>2</sub>/L-d, which is almost three times higher than that obtained in the present work. Conversely, Sganzerla et al. (2023) achieved a maximum HPR of 1.6 NL H<sub>2</sub>/L-d when evaluating the anaerobic co-fermentation of brewery by-products under thermophilic (55 °C) and acidogenic conditions (pH around 5). These values are almost 3.5 times lower than those obtained in the present study.

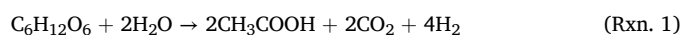
Remarkably, all the three HRT conditions exhibited high stability over the evaluation period (Table 4). Both stage I and II showed a similar HPSI of approximately 0.93. In stage III, where the HRT was 6 h, the recorded HPSI was of 0.97. To gain a comprehensive understanding of the BSG utilization, the YH<sub>dry-BSG</sub> (hydrogen yield in terms of mass of dry BSG) was analyzed across different HRTs. The YH<sub>dry-BSG</sub> values correlated directly with the shortening in HRT. The maximum YH<sub>dry-BSG</sub> achieved at a HRT of 12 h was 32.8 ± 2.2 NL H<sub>2</sub>/kg dry BSG, exceeding the values at HRTs of 9 and 6 h by 11.5 % and 36.5 %, respectively. Each ton of dry BSG could produce 20.8–32.8 m<sup>3</sup> of hydrogen depending on the HRT evaluated. Based on the highest heating value (HHV) of hydrogen (12.74 kJ/L), 264.9–417.8 MJ per ton of dry BSG could be obtained.

To the best of the authors' knowledge, there is no precedent for the operation of continuous DF reactors using BSG as a substrate. It is important to note that although the DF reactor was operated for only a few days, significantly different but stable HPRs were achieved in all the HRTs tested. This indicates that the HRT exerted a clear effect on the efficiency of fermentative hydrogen production in a continuous regime, where longer HRTs resulted in improved yields, while shorter HRTs increased hydrogen productivity. Future investigations should focus on

evaluating the long-term viability of the BSG DF process.

### 3.2.1. Profile of metabolites during hydrogen production

Soluble metabolites identified in the DF effluent for all operational stages included lactate, formate, acetate, propionate, butyrate, and isovalerate (Fig. 3). Initially, a significant concentration of lactate (3.9 g/L) was observed due to the batch start-up operation with lactose. During continuous operation, lactate, acetate, and butyrate dominated the metabolic profile. At 12 h HRT, the values were 2.0 ± 0.4, 2.3 ± 0.3, and 2.2 ± 0.4 g/L; at 9 h HRT, the values were 1.9 ± 0.1, 2.4 ± 0.3, and 3.6 ± 0.4 g/L; and finally, at 6 h HRT, the values were 2.1 ± 0.1, 2.2 ± 0.1, and 3.4 ± 0.2 g/L for lactate, acetate, and butyrate, respectively. The build-up of lactate is commonly linked to a impairment in hydrogen production, as suggested by previous studies (García-Depraect et al., 2021; Martínez-Mendoza et al., 2023). Throughout the study, lactate levels remained relatively low and did not appear to adversely affect hydrogen production. This may be explained by the type of inoculum used, which has the ability to convert lactate to hydrogen (Regueira-Marcos et al., 2023), thus ensuring continuous hydrogen production from BSG. On the other hand, the increased levels of acetate and butyrate during the prolonged HRT were consistent with the escalated HPR observed in stages II and III. The production of hydrogen via DF is commonly associated with the formation of butyrate and acetate, which result from the breakdown of carbohydrates, as described in Rxns. 1 and 2, respectively.



Theoretically, 4 moles of hydrogen are produced from 1 mol of glucose when acetate is the end product, while 2 moles of hydrogen are produced when butyrate is the end product. However, in mixed cultures, more efficient hydrogen production is often associated with the formation of butyrate as opposed to acetate. This preference is due to the potential acetogenesis/homoacetogenesis pathways leading to acetate, as observed in previous studies (García-Depraect et al., 2019). As for

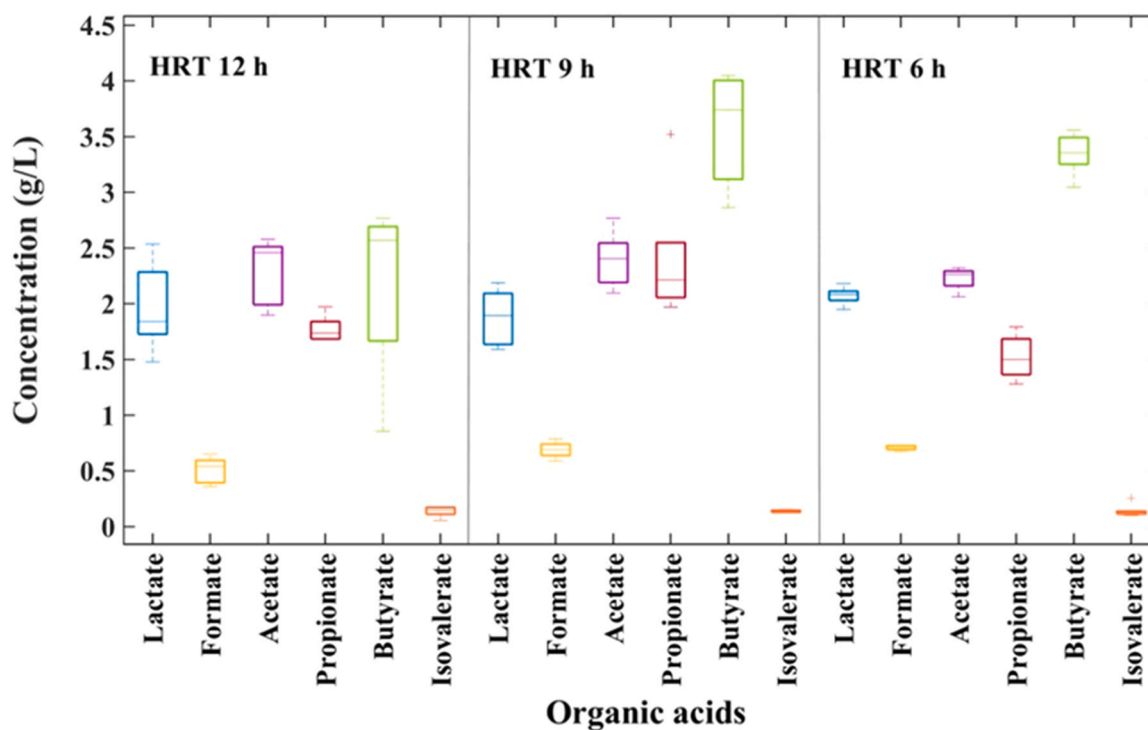
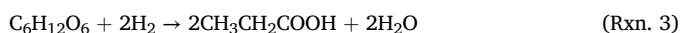


Fig. 3. Effect of HRT on the temporal dynamics of organic acid concentrations observed during the continuous fermentative production of hydrogen from pre-treated BSG.

propionate, its concentration in the acidogenic broth was  $1.8 \pm 0.1$ ,  $2.4 \pm 0.3$ , and  $1.5 \pm 0.2$  g/L for stages I, II, and III, respectively. Notably, stage II displayed a propionate concentration 60 % higher than that of stage III. The presence of propionate is conventionally associated with hydrogen consumption, suggesting a competitive reaction (Rxn. 3), as shown in previous research (García-Depraect et al., 2019). Finally, the recorded concentrations of formate and iso-valerate, specifically  $0.5 \pm 0.1$  and  $0.1 \pm 0.0$  g/L at a HRT of 12 h,  $0.7 \pm 0.1$  and  $0.1 \pm 0.0$  g/L at a HRT of 9 h, and  $0.7 \pm 0.0$  and  $0.1 \pm 0.0$  g/L at a HRT of 6 h, respectively, appear to have no discernible effect on hydrogen production.



### 3.2.2. Microbial communities in the hydrogen production reactor

Fig. 4a shows the bacterial assemblages identified during stable periods of hydrogen production at different HRTs. *Clostridium* emerged as

the predominant bacterial genus with relative abundances of 68, 87, and 98 % for HRTs of 12, 9, and 6 h, respectively. Despite the prevalence of *Clostridiales* species, 12 h HRT resulted in a more diverse microbiota, including *Enterobacteriales*, *Lachnospirales*, *Lactobacillales*, and *Eubacteriales* as subdominant taxa, representing 12, 5.6, 4.1, and 1.8 %, respectively. Different pathways for hydrogen production could be elucidated from the observed microbiota. For example, *Enterobacteria* follow a facultative anaerobic fermentation pathway, converting pyruvate to acetyl-CoA and formate via pyruvate formate lyase, leading to hydrogen production via the formate hydrogen lyase enzyme complex (Dzulkanain et al., 2022). In addition, a lactate-driven DF pathway may also occur, in which microorganisms, particularly those belonging to the genera *Clostridium* and *Lactobacillus*, produce lactate and further metabolize it to produce hydrogen (Aranda-Jaramillo et al., 2023; García-Depraect and León-Becerril, 2023). In addition, *Clostridium* spp. adhere to a strict anaerobic fermentation pathway involving the oxidation of pyruvate to acetyl-CoA and reduced ferredoxin by pyruvate

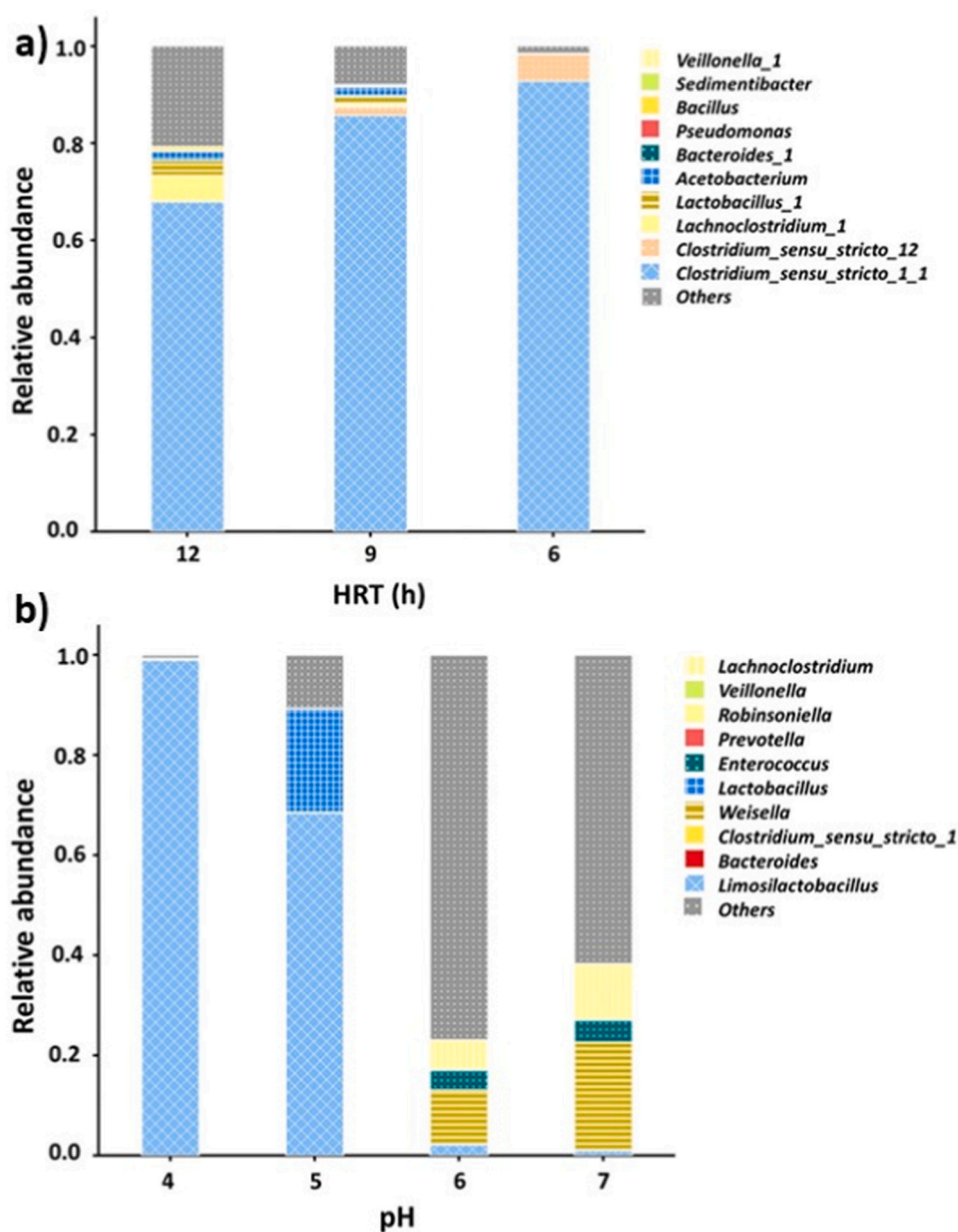


Fig. 4. Structure of the microbial community at the genus level in the acidogenic broth under different a) HRT and b) pH conditions. The category "Others" includes genera with a relative abundance below 1 %.

ferredoxin oxidoreductase (Dzulkanain et al., 2022). The exact hydrogen-producing pathways cannot be conclusively determined here. However, it can be hypothesized that the diversity of these pathways and their interactions contributed to a more efficient conversion of BSG hydrolysate to hydrogen.

### 3.3. Continuous production of organic acids from BSG acid-hydrolysate

The continuous production of organic acids entailed the utilization of acid hydrolysates derived from BSG at four different pH conditions, i.e., 4, 5, 6, and 7 (Fig. 5). At pH 4, the degree of acidification, calculated as the conversion of initial COD to organic acids, was 17 %. Lactic acid and acetic acid contributed 62.6 % ( $5.6 \pm 0.6$  g/L) and 32.1 % ( $1.9 \pm 0.3$  g/L), respectively, to this acidification process. At pH 4, formic, propionic, and butyric acids exhibited minimal concentrations (Table 5). It is worth noting that despite being storage at around 4 °C, the feeding displayed a consistently high concentration of lactic acid, averaging  $3.2 \pm 0.2$  g/L. Increasing the pH to 5 resulted in a rapid increase in the degree of acidification to 43.2 %, accompanied by variations in the organic acid profile, with an increase in propionic and butyric acids with concentrations of  $0.9 \pm 0.5$  and  $1.1 \pm 0.2$  g/L, respectively. Further adjustment of the pH to 6 led to an increase in the concentration of organic acids:  $9.2 \pm 0.7$ ,  $5.6 \pm 0.8$ ,  $1.6 \pm 0.2$ , and  $2.5 \pm 0.6$  g/L for lactic, acetic, propionic, and butyric acid, respectively. This resulted in a degree of acidification of 68.3 %, with a remarkable increase in the selectivity of 26.2 % for butyric acid. Finally, increasing the pH to 7 resulted in a decrease of the acidification degree to 37.4 %. Formic acid was produced at pH 7 reaching concentrations of  $1.4 \pm 0.1$  g/L, while the concentrations of acetic, propionic, and butyric acids remained at values of  $5.7 \pm 0.4$ ,  $1.4 \pm 0.1$ , and  $2.1 \pm 0.2$  g/L, respectively. Moreover, a significant decrease in lactic acid production was observed. This correlated with the increase in biogas productivity ( $1.4$  L/L-d with an average hydrogen composition of approximately 53 %) at pH 7. This observation is in line with the decrease in microbial communities responsible for lactic acid production discussed in the following Section 3.3.1. Thus, lactic acid might be implicated in hydrogen production pathways, as discussed in Section 3.2.1. This highlights the intricate interplay

between pH levels and the metabolic pathways governing various organic acids.

The pH exerts a considerable influence on anaerobic acidogenic performance and the preferential production of organic acids, primarily due to its impact on the microbial community and its associated metabolism (Bhatia et al., 2021). Over the range of pH conditions tested, the highest total organic acid production was observed at pH 6, reaching a maximum value of  $17.3 \pm 0.6$  g CODEquiv./L. In contrast, the lowest organic acid production occurred at pH 4, yielding  $4.3 \pm 0.2$  g CODEquiv./L. This finding is consistent with research by Da Fonseca et al. (2024), who also found that lower pH levels, such as pH 5, resulted in minimal organic acid production, specifically  $2.2 \pm 0.7$  g CODEquiv./L, in batch assays using BSG. In another study, Castilla-Archilla et al. (2021) investigated the production of VFAs using BSG at different pH conditions. The results revealed the highest VFAs concentration ( $17.0 \pm 1.3$  g CODEquiv./L) at pH 6.0, with significant selectivity (99.5–99.8 %) for acetate and butyrate. Similarly, Horiuchi et al. (2002) investigated the selective production of organic acids by anaerobic acidogenesis with pH control in a chemostat culture. Their findings also showed the lowest concentration of organic acid production at pH 5, with values reaching  $6.4$  g CODEquiv./L. A prevalence of lactic acid was observed at pH 4, while pH significantly influenced the composition of the active microbial communities, thereby influencing the pathways of organic acid production. Increasing the pH to 5 and 6 favored pathways related to butyric and propionic acids or the microbial communities associated with these acids.

The maximum concentration of organic acids obtained in the present study was  $17.3 \pm 0.6$  g CODEquiv./L, which was higher compared to the  $9.0 \pm 1.6$  g CODEquiv./L reported by Guarda et al. (2021), with a lab-scale expanded granular sludge bed reactor operated on pretreated (sulfuric acid) BSG in continuous mode at 30 °C, 2.5 days HRT, and 10 g COD/L-d OLR. In another study, Texeira et al. (2020) reported a maximum organic acid concentration of 35.5 g CODEquiv./L using a fed-batch reactor fed with from raw BSG and operated at an extended HRT of 16 days. However, the present study achieved a higher maximum organic acid productivity of  $900.5 \pm 13.1$  mg CODEquiv./L-h (six and ten times higher than the volumetric productivities reported by Guarda

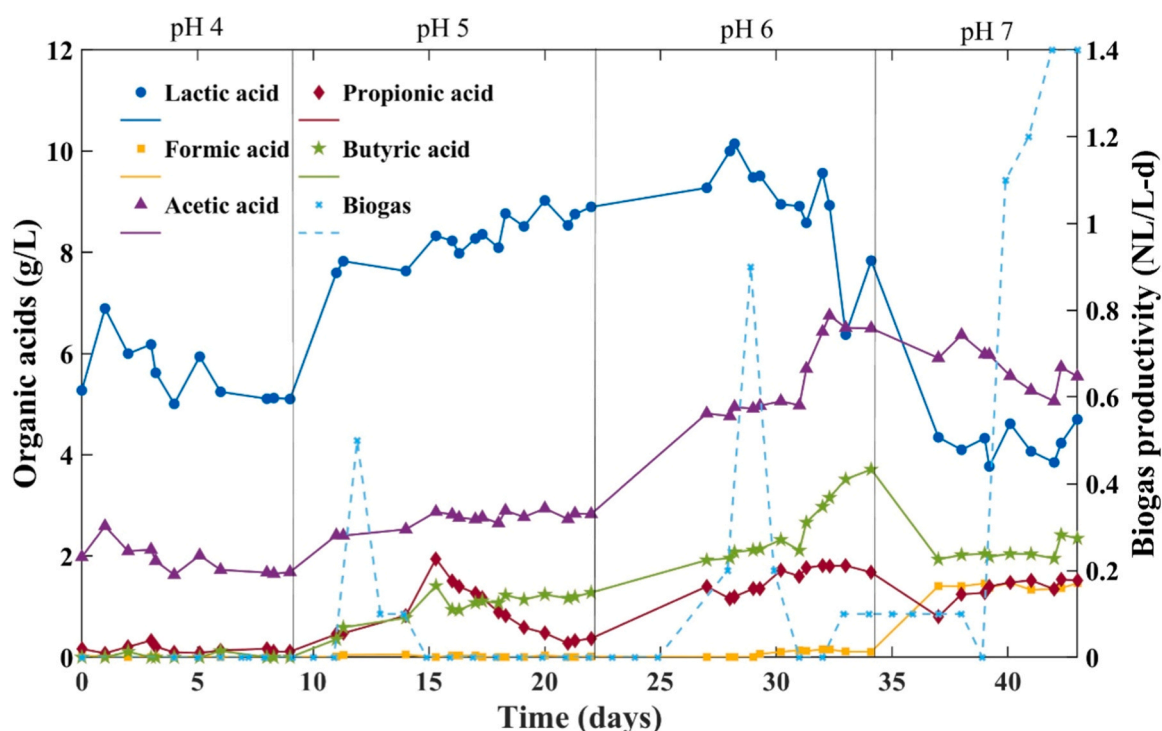


Fig. 5. Continuous production of carboxylic acids and biogas in the acidogenic reactor at different pH conditions.



**Table 5**

Organic acid concentrations, selectivity, and acidification degree were determined by COD-equivalent calculations using data obtained from the continuous reactor at different pH conditions.

	pH 4			pH 5			pH 6			pH7		
	[g/L] (influent)	[g/L] (effluent)	S (%)	[g/L] (influent)	[g/L] (effluent)	S (%)	[g/L] (influent)	[g/L] (effluent)	S (%)	[g/L] (influent)	[g/L] (effluent)	S (%)
Lactate	2.9 ± 0.1	5.6 ± 0.6	62.6 ± 8.4	2.8 ± 0.0	8.3 ± 0.4	53.5 ± 4.2	3.1 ± 0.1	9.2 ± 0.7	38.5 ± 3.2	4.2 ± 0.5	4.2 ± 0.3	5.2 ± 0.5
Formate	0.0 ± 0.0	0.0 ± 0.0	0.0 ± 0.0	0.0 ± 0.0	0.0 ± 0.0	0.0 ± 0.0	0.1 ± 0.1	0.1 ± 0.1	0.1 ± 0.0	0.0 ± 0.0	1.4 ± 0.1	5.1 ± 0.2
Acetate	0.7 ± 0.1	1.9 ± 0.3	32.1 ± 7.0	0.7 ± 0.0	2.7 ± 0.0	20.2 ± 1.6	0.8 ± 0.1	5.6 ± 0.8	29.2 ± 3.3	1.3 ± 0.1	5.7 ± 0.4	49.6 ± 4.5
Propionate	0.2 ± 0.1	0.2 ± 0.1	0.7 ± 0.0	0.2 ± 0.0	0.9 ± 0.5	8.7 ± 0.6	1.6 ± 0.3	1.6 ± 0.2	6.0 ± 0.9	1.5 ± 0.0	1.4 ± 0.1	0.0 ± 0.0
Butyrate	0.0 ± 0.0	0.0 ± 0.0	4.6 ± 0.7	0.0 ± 0.0	1.1 ± 0.2	17.6 ± 2.4	0.0 ± 0.0	2.5 ± 0.6	26.2 ± 4.7	0.0 ± 0.0	2.1 ± 0.2	40.1 ± 3.3
Acidification degree (%)		17.1 ± 0.8			43.2 ± 1.6			68.3 ± 2.4			37.4 ± 0.8	

S: selectivity

et al. 2021 and Texeira et al. (2020), respectively), highlighting the effective performance of the evaluated acidogenic process. Finally, the estimated organic acid yields, based on dry BSG, were 61.4 ± 2.9, 155.7 ± 5.7, 247.1 ± 8.6, and 135.7 ± 4.3 kg organic acids per ton of dry BSG for pH 4, 5, 6, and 7, respectively. The organic acids produced could serve as the basis for the synthesis of other compounds, such as polyhydroxyalkanoates (Guarda et al., 2021).

### 3.3.1. Microbial communities in the acidogenic reactor

In general, there was a predominant presence of *Lactobacillales* at both at pH 4 and pH 5, representing nearly 99 % of the relative abundance (Fig. 4b). Particularly at pH 4, the genus *Limosilactobacillus* showed a relative abundance of 98 %. Lactic acid bacteria, such as *Limosilactobacillus*, are widely known for their ability to perform lactic acid fermentation, yielding primarily lactic acid (Lee et al., 2023). However, certain strains of *Limosilactobacillus* and other lactic acid bacteria can also engage in additional metabolic pathways that result in the synthesis of other organic acids, such as acetic acid (Hirozawa et al., 2023). This finding is consistent with the increased levels of lactic and acetic acid observed at pH 4. A shift in pH to 5 resulted in a change in relative abundance, with *Limosilactobacillus* still predominant at 68 %, but with a notable presence of *Lactobacillus* at 20 % of relative abundance. *Lactobacillus*, in general, are known for their ability to perform lactic acid fermentation. However, some strains of *Lactobacillus* can also participate in mixed fermentations, contributing to the production of other organic acids (Hadinia et al., 2022).

The production of acetic, propionic, and butyric acids is a characteristic feature of heterofermentative lactic acid bacteria and other bacteria capable of performing mixed fermentation. These bacteria can use various metabolic pathways to ferment different substrates, resulting in the synthesis of different organic acids in addition to lactic acid, such as acetic acid. Shifting the pH to 6 resulted in an increased diversity of microbial communities and a significant reduction of *Lactobacillales* to 2 % (Fig. 4b). Subdominant genera such as *Weissella*, *Enterococcus*, and *Lachnospirillum* emerged, with relative abundances of 11 %, 4 %, and 6 %, respectively. While *Enterococcus* demonstrates metabolic versatility, it is commonly associated with lactic acid production along with *Weissella* (Heyer et al., 2024). In contrast, *Lachnospirillum*, which belongs to the family *Lachnospiraceae*, is associated with the production of short-chain fatty acids, including acetic, propionic, and butyric acids (Palomo-Briones et al., 2021). Many species within the genus *Lachnospirillum* are strict anaerobes and engage in carbohydrate fermentation, leading to the synthesis of these organic acids. In particular, certain strains of *Lachnospirillum* are known for their ability to produce butyric acid.

Finally, at pH 7, the relative abundance of *Weissella* and *Lachnospirillum* increased to 21 % and 11 %, respectively. While neither of these

genera is typically associated with hydrogen production, *Lachnospirillum* has the ability to generate small amounts of hydrogen as a by-product during certain fermentation processes. *Lachnospirillum* is closely associated with the hydrolysis of oligomers, which can promote hydrogen production (Palomo-Briones et al., 2021). On the other hand, *Clostridium sensu stricto 1* showed a low relative abundance (< 1 %) throughout the process. It is able to assimilate various types of feedstocks and convert them to hydrogen under different conditions (Yang and Wang., 2019), which may explain the peaks of hydrogen-containing biogas observed at pH 7.

### 3.4. Methane production from unfermented (CH<sub>4</sub>) and DF (H<sub>2</sub> + CH<sub>4</sub>) BSG hydrolysates

Both the unfermented BSG hydrolysates and the DF effluent collected under a 6 h HRT, which allowed maximum hydrogen production, were subjected to BMP tests. Following 12 days of methanization, the ultimate methane yield from the unfermented and fermented acid-hydrolysates were 516.8 ± 39.0 NmL CH<sub>4</sub>/g VS<sub>added</sub> and 658.4 ± 18.0 CH<sub>4</sub>/g VS<sub>added</sub>, respectively (Table 6). Commonly, DF has been reported to boost biogas production by stimulating hydrolysis and acidogenesis, resulting in increased concentrations of organic acids that are subsequently metabolized downstream. The acidogenic broth contained several organic acids, including lactate, acetate, formate, propionate, and butyrate, each present at concentrations in the range of a few grams per liter. However, no significant concentrations of these acids were detected in the GC-FID analysis performed on the acidogenic broth (data not shown), suggesting their use in biogas production. The final amount of

**Table 6**

Biochemical methane potential (BMP), along with the kinetic parameters derived from the modified Gompertz model, and the maximum volumetric methane production rates (VMPR) achieved for both the unfermented and fermented BSG hydrolysates.

Parameter	Unfermented hydrolysate	DF hydrolysate
BMP (NmL CH <sub>4</sub> /g VS <sub>added</sub> )	516.8 ± 39.0	658.4 ± 18.0
λ (days)	0.5	1.1
Hmax (NmL CH <sub>4</sub> /g VS <sub>added</sub> )	515.6	688.2
Rmax (NmL CH <sub>4</sub> /g VS <sub>added</sub> -d)	259.1	128.8
R <sup>2</sup>	0.9938	0.9977
VMPR (NmL CH <sub>4</sub> /L-d)	294.7	146.5

Hmax : Maximum methane production potential.

λ: Lag phase.

Rmax : Maximum rate of methane production.

R<sup>2</sup>: Correlation coefficient.

Values presented are the average and standard deviation of triplicate measurements.

lactate was not measured due to methodological limitations, but it is assumed that it underwent anaerobic oxidation to form methane precursors. As a result, the DF process acted as a pretreatment, leading to a 27.4 % increase in methane production compared to the unfermented counterpart. In both scenarios studied, the lag phase was relatively short (0.5–1.1 days), indicating the presence of readily assimilable organic compounds in the substrates (Fig. 6). Interestingly, while the acidogenic broth assay showed a higher production value, indicating an increase of 27 %, the volumetric methane production rates,  $R_{max}$ , decreased by almost 50 % compared to the fermented acid hydrolysate (Table 6). One possible reason for this could be that the microbiota of the anaerobic sludge used was adapted to metabolize low concentrations of organic acids. In this sense, a higher concentration of these compounds could imply some synthesis time for the cellular machinery needed to metabolize them. Therefore, in a continuous methanization process with adapted biomass, the difference in kinetics could be reduced.

With a focus on BSG utilization, the  $Y_{CH_4, dry-BSG}$  (methane yield relative to the mass of dry BSG) was analyzed for different hydrolysates. The highest  $CH_4 Y_{dry-BSG}$  was obtained when unfermented acid hydrolysates were used, with a yield of 226.9 NL  $CH_4$ /kg dry BSG. Conversely, the use of fermented acid hydrolysate resulted in a yield of 198.7 NL  $CH_4$ /kg dry BSG, representing a reduction of approximately 12 % due to the VS loss during DF. Considering the HHV of methane (35.2 kJ/L), unfermented acid hydrolysates have the potential to achieve an energy recovery yield of 7986.9 MJ/ton of dry BSG, while fermented acid hydrolysates could yield 6994.2 MJ/ton of dry BSG. To put the results of this study in the context of the current state of the art, Lins et al. (2023) achieved a methane yield of 580 NmL/g- $VS_{added}$  equivalent to approximately 82 NL  $CH_4$ /kg dry BSG in BMP batch tests for the mesophilic digestion of BSG at a F/M ratio of 1:3 (based on VS). In another study, Buller et al. (2022) reported lower methane yield of 107.3 NmL  $CH_4$ /g  $VS_{added}$  from BSG subjected to ultrasonic pretreatment in batch operation under mesophilic conditions and within a pH range of 7–8.

### 3.5. Significance of the study and the need for future research

The motivation for the present study was based on the following key points: i) the lack of previous research on continuous DF for the production of biohydrogen from BSG; ii) the scarcity of studies on continuous organic acid production using BSG as a substrate, with the microbiology of acidogenic processes for carboxylic acid production still largely unexplored; and iii) the BMP of the fermentation broths

produced after the DF process has, to the best of the authors' knowledge, not been previously investigated. The most notable results of this study include the fact that the volumetric hydrogen productivity obtained is the highest reported to date for pretreated BSG. In addition, the degree of acidification obtained was consistent with previous similar studies, but the volumetric carboxylic acid productivity obtained here was up to 10 times higher than that reported in other studies. In this context, the operating pH, which had not previously been studied in detail, was found to be an important parameter in the process. In addition, the microbiology associated with the continuous acidogenic process was determined, making this, to our knowledge, the second study to report and discuss such scientific findings in detail. It was also demonstrated that the effluent derived from the DF of BSG hydrolysates can be used for biogas production, where the methane production potential and kinetics were found to be quite attractive.

Overall, this research provides valuable insights into the optimization of fermentation processes for BSG and demonstrates its high potential as a low-cost feedstock for biohydrogen, carboxylic acids and methane. The results pave the way for future research aimed at improving the sustainability and profitability of the brewing industry by utilizing BSG for the production of renewable energy and valuable bio-based chemicals. In particular, deeper continuous studies with longer operating times are needed to further optimize these processes. In addition, a comprehensive techno-economic and environmental impact assessment is crucial to provide a more realistic view of the different biotechnological approaches explored here.

## 4. Conclusions

The continuous production of hydrogen and carboxylic acids from pretreated BSG and the batch methanization of unfermented and post-DF BSG hydrolysates were investigated. The DF process achieved the highest HPR of 5.9 NL- $H_2$ /L-d at 6 h HRT. pH significantly influenced the degree of acidification rather than the acid profile, with pH 6 producing the highest degree of acidification, yielding 247 kg of organic acids (mainly lactic and acetic acid) per ton of dry BSG. Both raw hydrolysates and DF hydrolysates showed a high methane production potential, 517 and 659 NmL- $CH_4$ /g- $VS_{added}$ , respectively. BSG has great potential as a low-cost feedstock for the production of biofuels and high-value chemicals.

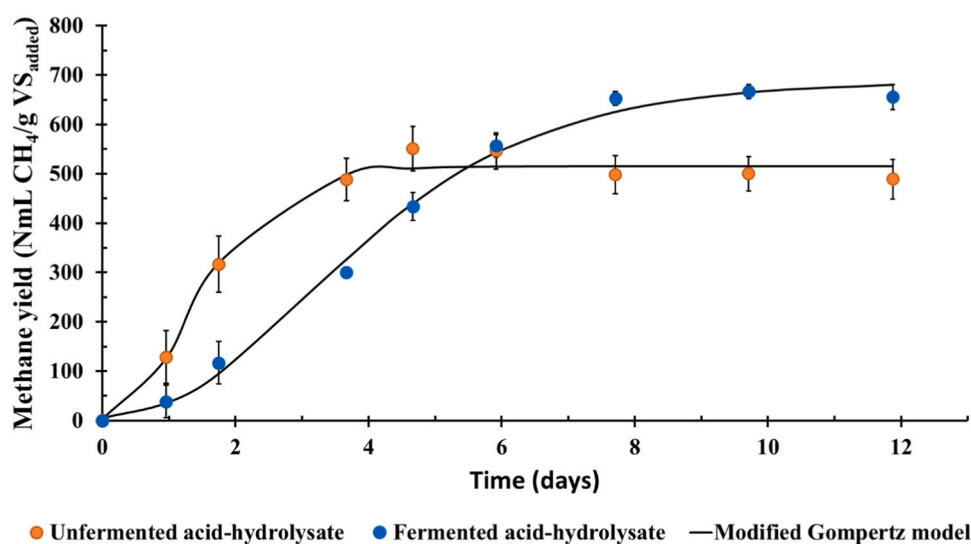


Fig. 6. Time course of the biochemical methane potential (BMP) for the unfermented BSG hydrolysates and the DF BSG hydrolysates. Error bars indicate the standard deviation of triplicate measurements.

## CRedit authorship contribution statement

**Jacobo Pérez-Barragán:** Writing – original draft, Methodology, Investigation. **Octavio García Depraect:** Writing – review & editing, Project administration, Methodology, Funding acquisition, Conceptualization. **Elizabeth León-Becerril:** Writing – review & editing, Supervision, Project administration, Funding acquisition. **Roberto Castro-Muñoz:** Writing – review & editing, Supervision. **Guillermo Quijano:** Resources. **Rafael Maya-Yescas:** Writing – review & editing, Supervision. **Cristina Martínez-Fraile:** Investigation. **Raúl Muñoz:** Writing – review & editing, Resources, Methodology.

## Declaration of Competing Interest

The authors declare that they have no known competing financial interests or personal relationships that could have appeared to influence the work reported in this paper.

## Acknowledgments

This research was funded by the Consejo Nacional de Humanidades, Ciencias y Tecnologías (CONAHCYT; Project-CF-2023-G648). The Grant RYC2021–034559-I funded by MCIN/AEI/10.13039/501100011033 and by the European Union NextGenerationEU/PRTR is also acknowledged. The Regional Government of Castilla y León and the European FEDER Programme (CL-EI-2021–07 and UIC 315) are also acknowledged. J. Pérez-Barragán acknowledges CONAHCYT for the Doctoral Scholarship 795519. The authors gratefully acknowledge the invaluable technical support provided by Beatriz Estfbalíz Muñoz-González, Araceli Crespo-Rodríguez, Enrique José Marcos-Montero and Daniel Fernández-Planillo.

## References

- Alonso-Riño, P., Amândio, M.S., Xavier, A.M., Beltrán, S., Sanz, M.T., 2022. Subcritical water as pretreatment technique for bioethanol production from brewer's spent grain within a biorefinery concept. *Polymers* 14 (23), 5218.
- APHA, 2005. Standard Methods for the Examination of Water and Wastewater (21st ed.). American Public Health Association/American Water Works Association/Water Environmental Federation, Washington, DC, USA.
- Aranda-Jaramillo, B., León-Becerril, E., Aguilar-Juárez, O., Castro-Muñoz, R., García-Depraect, O., 2023. Feasibility study of biohydrogen production from acid cheese whey via lactate-driven dark fermentation. *Fermentation* 9 (7), 644.
- Bhatia, S.K., Jagtap, S.S., Bedekar, A.A., Bhatia, R.K., Rajendran, K., Pugazhendhi, A., Yang, Y.H., 2021. Renewable biohydrogen production from lignocellulosic biomass using fermentation and integration of systems with other energy generation technologies. *Sci. Total Environ.* 765, 144429.
- Buller, L.S., Sganzerla, W.G., Lima, M.N., Muenchow, K.E., Timko, M.T., Forster-Carneiro, T., 2022. Ultrasonic pretreatment of brewers' spent grains for anaerobic digestion: Biogas production for a sustainable industrial development. *J. Clean. Prod.* 355, 131802.
- Castilla-Archilla, J., Papirio, S., Lens, P.N., 2021. Two-step process for volatile fatty acid production from brewery spent grain: hydrolysis and direct acidogenic fermentation using anaerobic granular sludge. *Process Biochem* 100, 272–283.
- Da Fonseca, Y.A., da Silva Barreto, E., Lomar, P.F., Silva, S.Q., Gurgel, L.V.A., Baêta, B.E. L., 2024. Biobased production of volatile fatty acids from brewer's spent grain: optimization and insights into the impact of protein extraction on process performance. *Biochem. Eng. J.* 203, 109218.
- Díaz-Cruces, V.F., García-Depraect, O., León-Becerril, E., 2020. Effect of lactate fermentation type on the biochemical methane potential of tequila vinasse. *Bioenergy Res* 13 (2), 571–580.
- Fernández-Delgado, M., Plaza, P.E., Coca, M., García-Cubero, M.T., González-Benito, G., Lucas, S., 2019. Comparison of mild alkaline and oxidative pretreatment methods for biobutanol production from brewer's spent grains. *Ind. Crops Prod.* 130, 409–419.
- García-Depraect, O., Castro-Muñoz, R., Muñoz, R., Rene, E.R., León-Becerril, E., Valdez-Vazquez, I., Buitrón, G., 2021. A review on the factors influencing biohydrogen production from lactate: the key to unlocking enhanced dark fermentative processes. *Bioresour. Technol.* 324, 124595.
- García-Depraect, O., Lebrero, R., Rodríguez-Vega, S., Börner, R.A., Börner, T., Muñoz, R., 2022. Production of volatile fatty acids (VFAs) from five commercial bioplastics via acidogenic fermentation. *Bioresour. Technol.* 360, 127655.
- García-Depraect, O., León-Becerril, E., 2023. Use of a highly specialized biocatalyst to produce lactate or biohydrogen and butyrate from agro-industrial resources in a dual-phase dark fermentation. *Fermentation* 9, 787.
- García-Depraect, O., Martínez-Mendoza, L.J., Díaz, I., Muñoz, R., 2022. Two-stage anaerobic digestion of food waste: enhanced bioenergy production rate by steering

- lactate-type fermentation during hydrolysis-acidogenesis. *Bioresour. Technol.* 358, 127358.
- García-Depraect, O., Muñoz, R., van Lier, J.B., Rene, E.R., Díaz-Cruces, V.F., León-Becerril, E., 2020. Three-stage process for tequila vinasse valorization through sequential lactate, biohydrogen and methane production. *Bioresour. Technol.* 307, 123160.
- García-Depraect, O., Osuna-Laveaga, D.R., León-Becerril, E., 2019. A Comprehensive Overview of the Potential of Tequila Industry By-Products for Biohydrogen and Biomethane Production: Current Status and Future Perspectives. *New Advances on Fermentation Processes*. IntechOpen.
- Giacobbe, S., Piscitelli, A., Raganati, F., Lettera, V., Sannia, G., Marzocchella, A., Pezzella, C., 2019. Butanol production from laccase-pretreated brewer's spent grain. *Biotechnol. Biofuels* 12, 1–8.
- Guarda, E.C., Oliveira, A.C., Antunes, S., Freitas, F., Castro, P.M., Duque, A.F., Reis, M.A., 2021. A two-stage process for conversion of brewer's spent grain into volatile fatty acids through acidogenic fermentation. *Appl. Sci.* 11 (7), 3222.
- Hadinia, N., Dovom, M.R.E., Yavarmansh, M., 2022. The effect of fermentation conditions (temperature, salt concentration, and pH) with lactobacillus strains for producing short chain fatty acids. *LWT* 165, 113709.
- Hejna, A., Barczewski, M., Skórczewska, K., Szulc, J., Chmielnicki, B., Korol, J., Formela, K., 2021. Sustainable upcycling of brewers' spent grain by thermo-mechanical treatment in twin-screw extruder. *J. Clean. Prod.* 285, 124839.
- Heyer, C.M.E., Dörper, A., Sommerfeld, V., Gänzle, M.G., Zijlstra, R.T., 2024. Effect of acidification or fermentation of barley grain using *Limosilactobacillus reuteri* or *Weissella cibaria* on inositol phosphate hydrolysis in vitro. *Anim. Feed Sci. Technol.* 309, 115887.
- Hirozawa, M.T., Ono, M.A., de Souza Suguiura, I.M., Garcia, S., Bordini, J.G., Amador, I. R., Ono, E.Y.S., 2023. *Limosilactobacillus reuteri* as sustainable biological control agent against toxigenic *Fusarium verticillioides*. *Braz. J. Microbiol.* 54 (3), 2219–2226.
- Kiring Holdings, 2021. Beer consumption by region (Year) Available online: [https://www.kiringholdings.com/en/investors/library/databook/beer\\_region/](https://www.kiringholdings.com/en/investors/library/databook/beer_region/) (accessed on 6 May 2024).
- Horiuchi, J.I., Shimizu, T., Tada, K., Kanno, T., Kobayashi, M., 2002. Selective production of organic acids in anaerobic acid reactor by pH control. *Bioresour. Technol.* 82 (3), 209–213.
- Kumar, G., Sivagurunathan, P., Park, J.H., Park, J.H., Park, H.D., Yoon, J.J., Kim, S.H., 2016. HRT dependent performance and bacterial community population of granular hydrogen-producing mixed cultures fed with galactose. *Bioresour. Technol.* 206, 188–194.
- Lee, B.H., Shih, M.K., Hou, C.Y., 2023. New insights into the application of lactic acid bacterial strains in fermentation 2.0. *Fermentation* 9 (10), 868.
- Li, J., Tao, H., 2016. Microwave-assisted HCl pretreatment of brewers' spent grain to promote hydrogen production in dark fermentation. *Kezaisheng Nengyuan/ RES* 34 (9), 1391–1397.
- Liang, S., Wan, C., 2015. Carboxylic acid production from brewer's spent grain via mixed culture fermentation. *Bioresour. Technol.* 182, 179–183.
- Lins, L.P., Martinez, D.G., Furtado, A.C., Padilha, J.C., 2023. Biomethane generation and CO<sub>2</sub> recovery through biogas production using brewers' spent grains. *Biocatal. Agric. Biotechnol.* 48, 102579.
- Liu, C., Ullah, A., Gao, X., Shi, J., 2023. Synergistic ball milling–enzymatic pretreatment of brewer's spent grains to improve volatile fatty acid production through thermophilic anaerobic fermentation. *Processes* 11 (6), 1648.
- Marín, D., Méndez, L., Suero, I., Díaz, I., Blanco, S., Fdz-Polanco, M., Muñoz, R., 2022. Anaerobic digestion of food waste coupled with biogas upgrading in an outdoors algal-bacterial photobioreactor at pilot scale. *Fuel* 324, 124554.
- Martínez-Mendoza, L.J., García-Depraect, O., Muñoz, R., 2023. Unlocking the high-rate continuous performance of fermentative hydrogen bioproduction from fruit and vegetable residues by modulating hydraulic retention time. *Bioresour. Technol.* 373, 128716.
- Pabbathi, N.P.P., Velidandi, A., Pogula, S., Gandam, P.K., Baadhe, R.R., Sharma, M., Gupta, V.K., 2022. Brewer's spent grains-based biorefineries: A critical review. *Fuel* 317, 123435.
- Palomo-Briones, R., de Jesús Montoya-Rosales, J., Razo-Flores, E., 2021. Advances towards the understanding of microbial communities in dark fermentation of enzymatic hydrolysates: diversity, structure and hydrogen production performance. *Int. J. Hydrog. Energy* 46 (54), 27459–27472.
- Patel, A., Mikes, F., Bühler, S., Matsakas, L., 2018. Valorization of brewers' spent grain for the production of lipids by oleaginous yeast. *Molecules* 23 (12), 3052.
- Rachwał, K., Waško, A., Gustaw, K., Polak-Berecka, M., 2020. Utilization of brewery wastes in food industry. *PeerJ* 8, e9427.
- Regueira-Marcos, L., Muñoz, R., García-Depraect, O., 2023. Continuous lactate-driven dark fermentation of restaurant food waste: process characterization and new insights on transient feast/famine perturbations. *Bioresour. Technol.* 129385
- Rojas-Chamorro, J.A., Romero, I., López-Linares, J.C., Castro, E., 2020. Brewer's spent grain as a source of renewable fuel through optimized dilute acid pretreatment. *Renew. Energy* 148, 81–90.
- Sahrin, N.T., Khoo, K.S., Lim, J.W., Shamsuddin, R., Ardo, F.M., Rawindran, H., Cheng, C.K., 2022. Current perspectives, future challenges and key technologies of biohydrogen production for building a carbon-neutral future: a review. *Bioresour. Technol.* 364, 128088.
- Salangsang, M.C.D., Sekine, M., Akizuki, S., Sakai, H.D., Kurosawa, N., Toda, T., 2022. Effect of carbon to nitrogen ratio of food waste and short resting period on microbial accumulation during anaerobic digestion. *Biomass-- Bioenergy* 162, 106481.
- Sarkar, O., Rova, U., Christakopoulos, P., Matsakas, L., 2021. Influence of initial uncontrolled pH on acidogenic fermentation of brewery spent grains to biohydrogen

- and volatile fatty acids production: optimization and scale-up. *Bioresour. Technol.* 319, 124233.
- Sarkar, O., Rova, U., Christakopoulos, P., Matsakas, L., 2022. Effect of metals on the regulation of acidogenic metabolism enhancing biohydrogen and carboxylic acids production from brewery spent grains: microbial dynamics and biochemical analysis. *Eng. Life Sci.* 22 (10), 650–661.
- Sganzerla, W.G., Sillero, L., Forster-Carneiro, T., Solera, R., Perez, M., 2023. Determination of anaerobic co-fermentation of brewery wastewater and brewer's spent grains for bio-hydrogen production. *Bioenergy Res.* 16 (2), 1073–1083.
- Sluiter, A., Hames, B., Ruiz, R., Scarlata, C., Sluiter, J., Templeton, D., Crocker, D., 2008. Determination of Structural Carbohydrates and Lignin in Biomass: Laboratory Analytical Procedure (LAP) (Revised July 2022). [http://www.nrel.gov/biomass/analytical\\_procedures.html](http://www.nrel.gov/biomass/analytical_procedures.html).
- Soares, J.F., Mayer, F.D., Mazutti, M.A., 2024. Hydrogen production from brewer's spent grain hydrolysate by dark fermentation. *Int. J. Hydrog. Energy* 52, 352–363.
- Statista Search Department, 2022. Beer production worldwide by region, <https://www.statista.com/statistics/202417/beer-output-volumes-of-the-different-continent-in-2020>. (Accessed on 6 May 2024).
- Teixeira, M.R., Guarda, E.C., Freitas, E.B., Galinha, C.F., Duque, A.F., Reis, M.A., 2020. Valorization of raw brewers' spent grain through the production of volatile fatty acids. *N. Biotechnol.* 57, 4–10.
- Wagner, E., Sierra-Ibarra, E., Rojas, N.L., Martinez, A., 2022. One-pot bioethanol production from brewery spent grain using the ethanologenic *Escherichia coli* MS04. *Renew. Energy* 189, 717–725.
- Woon, J.M., Khoo, K.S., Al-Zahrani, A.A., Alanazi, M.M., Lim, J.W., Cheng, C.K., Kiatkittipong, W., 2023. Epitomizing biohydrogen production from microbes: Critical challenges vs opportunities. *Environ. Res.* 227, 115780.
- Yang, G., Wang, J., 2019. Changes in microbial community structure during dark fermentative hydrogen production. *Int. J. Hydrog. Energy* 44 (47), 25542–25550.
- Zeko-Pivač, A., Tišma, M., Žnidaršič-Plazl, P., Kulisic, B., Sakellaris, G., Hao, J., Planinić, M., 2022. The potential of brewer's spent grain in the circular bioeconomy: State of the art and future perspectives. *Front. Bioeng. Biotechnol.* 10, 870744.
- Zhang, J., Zang, L., 2016. Enhancement of biohydrogen production from brewers' spent grain by calcined-red mud pretreatment. *Bioresour. Technol.* 209, 73–77.